Techno-Economic Comparison of SOEC based Hydrogen Production with Large PWRs and SMRs in S. Korea

*Changmin Yoon[ab], Jeong Ik Lee[a]**
[a]Nuclear Quantum Engineering department, KAIST, Yuseong-gu, Daejeon, 34141
**Corresponding author: jeongiklee@kaist.ac.kr*

***Keywords: Solid oxide electrolysis cell, Nuclear hydrogen, Techno-economic analysis, Small modular reactor, Hydrogen supply chain**

1. Introduction

The urgent global challenge to combat climate change and global warming is the need to secure clean energy sources to replace fossil fuels. Among these sources, hydrogen is becoming increasingly important as a key energy carrier for next-generation energy systems due to its high energy density, environmentally friendly characteristics, and ease of storage and transportation. Its importance is particularly growing in industries where reducing carbon emissions is essential, such as oil refining and steelmaking [1]. In these industries, hydrogen can be used directly as a fuel and a reducing agent. The South Korean government has also taken steps to promote hydrogen as a key component in its strategy to reduce national greenhouse gas emissions. The government has actively pursued medium- to long-term plans to increase the supply of hydrogen and ensure its affordability by creating legal and institutional frameworks, including the "Hydrogen Economy Roadmap (2019)" and the "Hydrogen Economy Promotion and Hydrogen Safety Management Act (2020)" [2,3]. To achieve these goals, nuclear-coupled hydrogen production technology is considered as a crucial alternative for the stable and economical production of large quantities of clean hydrogen [4].

Water electrolysis technologies for hydrogen production are primarily classified as alkaline water electrolysis (AWE), polymer electrolyte membrane (PEM) electrolysis, or solid oxide electrolysis cells (SOEC). SOEC technology has the advantage of significantly higher hydrogen production efficiency than other technologies because a portion of the electrical energy required for electrolysis can be substituted with thermal energy. SOECs generally operate in high-temperature environments between 750°C and 900°C [5]. However, recent research and development by various commercial SOEC module manufacturers has demonstrated that efficient electrolysis is possible when supplied with steam at around 200°C [6]. This is achieved by absorbing internal waste heat within the modules. This suggests that SOEC electrolysis systems can be effectively coupled with Pressurized Water Reactor (PWR) types, which operate at lower temperatures.

Implementing a highly competitive hydrogen economy requires an exhaustive cost evaluation from a life-cycle framework. This evaluation must encompass not only "plant-gate" production, but also delivery to final demand sites. Because hydrogen has a low volumetric energy density, transporting the produced gas to demand centers requires capital-intensive infrastructure, such as high-pressure compression and extensive pipeline networks [7]. The costs of this compression and transmission infrastructure account for a significant portion of the ultimate levelized cost of hydrogen (LCOH). Since the capital expenditure (CAPEX) for pipeline delivery is sensitive to transmission distance and target hydrogen demand, assessing the practical feasibility of a nuclear-hydrogen system requires an integrated supply chain perspective rather than only considering production costs.

To commercialize systems that integrate nuclear energy with SOEC technology, a comprehensive techno-economic analysis is required to identify the optimal supply architecture. The objective of this study is to thermodynamically design and analyze SOEC hydrogen production systems coupled with a large-scale PWR and an integral PWR type Small Modular Reactors (SMRs). Based on the derived thermodynamic performance, a rigorous life-cycle economic analysis is conducted, incorporating Monte Carlo simulations for uncertainties in capital costs, compression, and pipeline transmission variables. Ultimately, this research identifies the break-even distances and demand scales at which localized i-PWRs are more economically feasible than centralized large-scale NPPs, providing quantitative guidelines for future clean hydrogen supply strategies.

Therefore, in order to commercialize systems that combine nuclear energy with SOEC electrolysis technology, it is necessary to thoroughly examine the life-cycle economics. This includes determining the amount of hydrogen that each reactor type can produce and calculating the final supply unit cost. This study aims to design systems that produce hydrogen by coupling large PWRs and SMRs with SOEC electrolysis technology and to conduct detailed thermodynamic analyses of these systems. Furthermore, a life-cycle economic analysis is conducted, incorporating compression and transportation, based on the derived thermodynamic performance results. This analysis deduced the practical competitiveness of each technology and system across varying transport distances and the optimal hydrogen supply strategy.

2. Methodology

This study defines the life-cycle LCOH as the sum of production, compression, and transmission costs, as expressed in Eq. (1).

$$LCOH_{\text{life-cycle}} = LCOH_{\text{production}} + LCOH_{\text{compression}} + LCOH_{\text{transmission}} \quad (1)$$

Each component of the LCOH is derived based on economic parameters and thermodynamic modeling results. The target nuclear energy systems evaluated in this analysis are a large-scale NPP with a capacity of 1400 MWe and an SMR with a capacity of 170 MWe (i-PWR). For this analysis, it was assumed that the nuclear power plant fully supplied the electricity required for the entire process, including water electrolysis and compression.

2.1. Thermodynamic modeling

Life-cycle thermodynamic modeling was conducted to determine the hydrogen production rate and estimate capital expenditures for the equipment used in each process. The SOEC used in this study requires electrical and thermal energy, necessitating complex thermal integration modeling with the nuclear reactor. Thus, an integrated model was developed that includes the nuclear-coupled SOEC system, the hydrogen compression system, and the transmission system to the demand site.

2.1.1. Hydrogen production system

Modeling of the power conversion system was conducted for each respective reactor. For the large-scale NPP, the modeling was based on the United States Nuclear Regulatory Commission (US-NRC) design control document for the APR1400 [8]. For the PWR type small modular reactor (i-PWR), the system was modeled based on the Final Safety Analysis Report from NuScale Power alongside US-NRC data [9]. The specific modeling parameters for the nuclear systems are outlined in Table 1 and Table 2. The layouts of the integrated SOEC systems for each reactor type are illustrated in Fig. 1 and Fig. 2.

Table 1. Modeling parameters of large-scale NPP

Parameters	Value
Thermal input power	$3985MW_{th}$
Net electricity	1400 MWe
Turbine efficiency	90%
Pump efficiency	80%
Generator efficiency	96%
Reheater effectiveness	95%
Reheater pressure drop	3%
SG outlet temperature	282.2℃
SG outlet pressure	6.633MPa

Table 2. Modeling parameters of i-PWR

Parameters	Value
SG thermal power	520MWth
Net electricity	176.5 MWe
Turbine efficiency	90%
Pump efficiency	80%
Reboiler effectiveness	95%
Hot side pressure drop	3%
Cold side pressure drop	3%
Turbine extraction fraction	7%

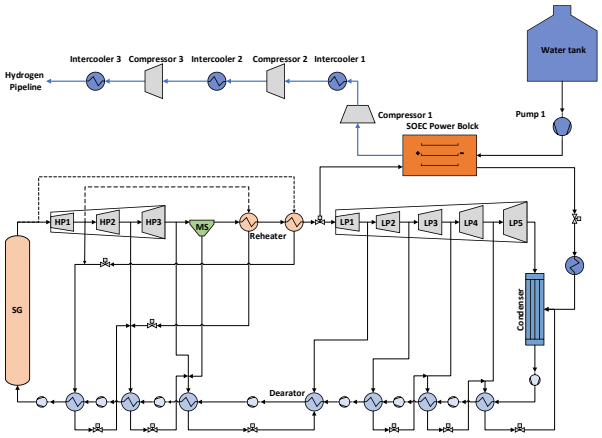

Figure 1. Layout of integrated large-scale NPP with SOEC

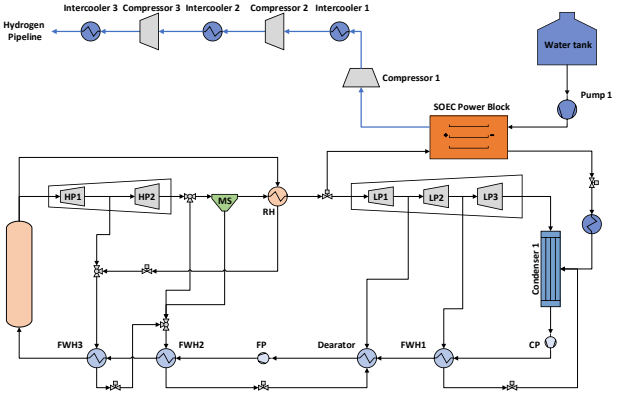

Figure 2. Layout of integrated i-PWR with SOEC

The SOEC system was modeled utilizing data from the Idaho National Laboratory, incorporating the SOE power block, the air sweep system, and the hydrogen purification system [10]. The specific parameters applied to SOEC modeling are presented in Table 3. The hydrogen production efficiency was calculated to evaluate the overall performance of the integrated nuclear-hydrogen system. In this integrated system, the total efficiency (η_{total}) is defined as the ratio of the

energy content of the produced hydrogen to the total thermal energy generated by the nuclear reactor. The efficiency can be expressed as follows:

$$\eta_{total} = \frac{\dot{m}_{H_2} \cdot LHV_{H_2}}{\dot{Q}_{reactor}}$$

where $\dot{m}_{H_2}$ is the mass flow rate of the produced hydrogen, LHV_{H_2} is the lower heating value of hydrogen, and $\dot{Q}_{reactor}$ is the total thermal power generated by the nuclear reactor, representing the total energy input to the integrated system.

Table 3. Modeling parameters of SOEC system [10]

Parameter	Value
Stack operating temperature	800 °C
Stack operating pressure	5 bars
Operating mode	Constant V
Cell voltage	1.29 V/cell
Current density	1.0 A/cm²
Stack inlet H_2O composition	90 mol%
Steam utilization	80%
HTSE modular-block capacity	25 MW-dc
Cell area per modular block	1945.4 m²
Sweep gas	Air
Sweep-gas inlet flow rate	Flow set to achieve 40 mol% O_2 in anode outlet stream
Reboiler pinch temperature	20K
Recuperator pinch temperature	15K

2.1.2. Hydrogen compression system

Depending on the targeted transmission method, hydrogen must be pressurized to 70 bar prior to delivery to the demand site. To avoid the high discharge temperatures associated with single-stage compression, which would exceed the API 618 maximum limit of 120°C, a multi-stage compression configuration with intercoolers was modeled [11]. The required number of stages (N) and the stage pressure ratio (r_*) were calculated using the first law of thermodynamics under the assumptions of an ideal gas and a reversible adiabatic process. These mathematical formulations are expressed in Eq. (2) - (4).

$$T_{out} = T_{in}\left(1 + \frac{\left(\frac{P_{out}}{P_{in}}\right)^{\frac{\gamma-1}{\gamma}} - 1}{\eta_c}\right), \gamma = \frac{c_p}{c_v} \quad (2)$$

$$r_* = [1 + \eta_c(\frac{T_{max}}{T_{in}} - 1)]^{\frac{\gamma}{\gamma-1}} \quad (3)$$

$$N = \left[\frac{\ln\left(\frac{P_{out}}{P_{in}}\right)}{\ln(r_*)}\right], r_* \approx \left(\frac{P_{out}}{P_{in}}\right)^{\frac{1}{N}} \quad (4)$$

2.1.3. Hydrogen transmission system

This study evaluates pipeline transmission strategies for the large-scale NPP and the i-PWR. It considers pipelines with varying capacities, which are designed according to the scale of hydrogen demand. Due to internal friction-induced pressure losses and the operational requirement to maintain a minimum pressure threshold (P_{min}), evaluating pipeline transmission demands a detailed analytical approach. To evaluate the maximum allowable pipeline length (L_{max}) before requiring intermediate booster compressors, the Darcy–Weisbach equation (Eq. (5)) was used. The maximum pipeline diameter was set at 16 inches based on commercial standards and velocity limits: an inlet velocity below 10 m/s and an internal flow velocity capped at 20 m/s.

$$\frac{dP}{dx} = -f\frac{\rho V^2}{2D}, \dot{m} = \rho A, \quad A = \frac{\pi D^2}{4}, \quad \rho = \frac{P\,M}{ZRT} \quad (5)$$

The Darcy-Weisbach equation is analytically integrated by imposing assumptions of isothermal flow, uniform pipe roughness, and constant fluid viscosity. This yields the maximum achievable transmission distance (L_{max}), without additional compression, as shown in Eq. (6).

$$L_{max} = \frac{(P_{in}^2 - P_{min}^2)\, D\, A^2}{f\, \dot{m}^2\, Z\, R_s\, T} \quad (6)$$

As a result, in scenarios where the overall transport distance (L) remains within L_{max}, the system is modeled without secondary compression. If L exceeds this calculated limit, installing booster compressors along the pipeline network is presumed to restore the necessary hydrogen pressure. Table 4 summarizes all the fundamental thermodynamic parameters for compression and transmission systems.

Table 4. Modeling parameters of compression and transmission system.

Properties	Design Value
Isentropic efficiency (η_{is})	0.88 [12]
Motor efficiency (η_{motor})	0.94 [12]
P_{min}	600 psig
P_{in}	70 bar
μ	$8.9 \cdot 10^{-6} Pa \cdot s$
ε	$4.5 \cdot 10^{-5} m$

z	1.05
R_s	$0.082\ L \cdot atm/(mol \cdot K)$
f	Swamee–Jain equation

2.1.4. Integrated system

Integrating the SOEC system with the nuclear power plant requires steam to be extracted upstream of the low-pressure turbine (LPT) to provide process heat. This extraction inherently induces off-design operating conditions in the secondary cycle, so a comprehensive off-design modeling framework was developed for the key power conversion components. The off-design behavior of the steam turbine, specifically the flow-pressure correlation and the isentropic efficiency of the final stage, was evaluated using Stodola's law and the Ray equation, respectively. Additionally, the performance deviation of the feedwater heaters due to reduced extraction steam was modeled using the ε-NTU method under the assumption of a constant overall heat transfer coefficient (UA). Finally, to stabilize the reactor-side boundary conditions, a control strategy was implemented to keep the steam generator (SG) inlet feedwater temperature at its design point. SG inlet feedwater temperature drop caused by reduced feedwater heating is assumed to be offset by additional steam extraction downstream of the high-pressure turbine.

2.2. Economic analysis modeling

This study evaluates the life-cycle LCOH as a function of distance transmission to assess the economic competitiveness of different transport scenarios. Comprehensive LCOH was determined by aggregating constituent expenses across successive phases of hydrogen production, compression, and delivery. A Monte Carlo simulation was executed to address the inherent uncertainties associated with critical, capital-intensive input parameters. Each economic parameter, identified by an asterisk (*) in the tables, was assumed to follow a triangular distribution with a ±20% uncertainty margin relative to its baseline estimate. A total of 50,000 sampling iterations were performed to ensure the statistical robustness of the results.

To normalize cost figures from various literature sources, all financial data were standardized to 2024 USD. CAPEX was escalated using the Chemical Engineering Plant Cost Index (CEPCI), while labor-dependent operation and maintenance (O&M) expenses were updated using the Unit Labor Cost (ULC) index. An exchange rate of 1,400 KRW/USD was applied to standardize the current-year data.

2.2.1. Hydrogen production cost

The LCOH for production was calculated by including all expenses associated with the nuclear power plant that generates energy and the electrolysis facility that produces hydrogen. Due to the different design lifetimes of the primary components, 60 years for the nuclear reactor, 20 years for the electrolysis balance of plant (BOP), and seven years for the electrolyzer stack—the reinvestment expenditures for equipment with shorter replacement cycles were converted to their present value (PV) and included in the overall economic assessment.

$$LCOH_{production} = \frac{\left(TCI_{NPP} + \sum_{t=1}^{N} \frac{\mathrm{O\&M_{NPP}} + \mathrm{Fuel_{NPP}} + \mathrm{De_{NPP}} + \mathrm{P\&G_{NPP}} + \mathrm{W_{NPP}}}{(1+r)^t} + PV_{stack} + PV_{BOP} + \sum_{t=1}^{N} \frac{\mathrm{O\&M_{EL}} + \mathrm{Fuel_{EL}}}{(1+r)^t}\right)}{\sum_{t=1}^{N} \frac{H_{2,t}}{(1+r)^t}} \quad (7)$$

The nuclear cost model incorporates capital investment, O&M, fuel, and decommissioning costs, as well as socio-political indirect costs. The SOEC system's total capital investment (TCI) is evaluated using a specific cost correlation method that distinguishes between scalable and modular components. Detailed economic parameters, decommissioning costs, and SOEC TCI correlation factors are provided in Appendix A.

2.2.2. Hydrogen compression cost

Hydrogen produced via electrolysis is pressurized to 70 bar to meet the operational requirements for pipeline transmission. The CAPEX for compressors is calculated based on motor ratings and cost correlations derived from the HDSAM framework. To align with the nuclear plant's 60-year operational lifetime, periodic reinvestment for compression equipment is discounted to its PV and included in the total economic assessment. Specific mathematical formulations for intercooler CAPEX and foundational design variables for the compression system are detailed in Appendix B.

$$LCOH_{compression} = \frac{PV_{\mathrm{compression}} + \sum_{t=1}^{N} \frac{\mathrm{O\&M_{compression}}}{(1+r)^t}}{\sum_{t=1}^{N} \frac{H_{2,t}}{(1+r)^t}} \quad (8)$$

2.2.3. Hydrogen transmission cost

The transmission LCOH is evaluated based on a pipeline methodology, with capacity designed according to the target hydrogen demand. This assessment includes the CAPEX for pipeline installation and the procurement of booster compressors to overcome friction-induced pressure drops. Regarding hydrogen loss, a mass loss of 0.5% is assumed for each booster stage to account for dynamic seal leakage and venting. Operational costs are determined using 2024 electricity grid SMP data. Detailed pipeline unit costs and specific transmission economic parameters are presented in Appendix C.

$$LCOH_{trans,pipe} = \frac{TCI_{\text{pipeline}} + PV_{\text{compressor}} + \left(\sum_{t=1}^{N} \frac{\text{O\&M}_{\text{pipeline+compressor}} + \text{Fuel}_{\text{compressor}}}{(1+r)^t}\right)}{\sum_{t=1}^{N} \frac{H_{2,t}}{(1+r)^t}} \quad (9)$$

3. Results

3.1. Thermodynamic analysis results

A study was conducted to determine the operating conditions for the integrated system by varying the steam extraction fraction upstream of the LPT. Since comprehensive thermodynamic optimization is beyond the scope of this economic study, the analysis focused on identifying the operating point that maximizes the hydrogen production rate. The resulting thermodynamic performance parameters at these optimal conditions are summarized in Table 5 for the three evaluated scenarios. Large-scale NPP configurations achieve maximum hydrogen production rates of 10.87 kg/s, with overall efficiencies approaching 34%. In contrast, the i-PWR scenario yields a production rate of 1.34 kg/s with an efficiency of 31.07%. This difference in efficiency is due to the higher baseline thermal efficiencies of large-scale NPP power conversion systems compared to those of SMR. The system capacities, compression work, and energy consumption profiles derived from these maximized production conditions serve as the baseline for the subsequent life-cycle economic evaluation.

Table 5. Thermodynamic results for maximum hydrogen production

	Large-scale NPP +Pipeline	**i-PWR + Pipeline**
Hydrogen production (kg/s)	10.87	1.39
Hydrogen production (k-ton/year)	291.4	35.9
Electrolyzer stack capacity (MW)	1269.1	162.3
Electrolyzer BOP power (MW)	11.16	0.83
Compressor work (MW)	44.14	5.63
Compression stage number	3	3
Hydrogen production efficiency (%)	34.16	32.15

3.2. Economic analysis results

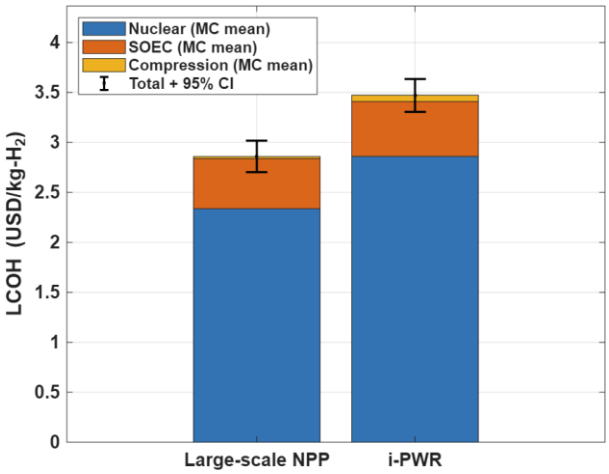

Figure 3. Breakdown of the LCOH for production and compression

Figure 3 shows a comparison of the components of the LCOH for the large-scale NPP and i-PWR at the production and primary compression stages, excluding long-distance pipeline transmission. Each bar represents the contribution of the nuclear power plant, SOEC, and compression sectors, based on average Monte Carlo simulation values. The error bars indicate the 95% confidence interval of the total cost. The analysis results show that the average LCOH at the plant gate for the large-scale NPP is approximately [2.86 ± 0.16] USD/kg-H_2, demonstrating clear cost competitiveness compared to the i-PWR, evaluated at around [3.47 ± 0.16] USD/kg-H_2. The most critical factor driving this cost difference is the cost gap in the nuclear sector. The large-scale NPP achieves strong economies of scale based on its substantial 1,400 MWe output. This results in lower overnight and O&M costs per unit of electricity.

In contrast, the 170 MWe i-PWR has a higher capital cost per unit of output due to its smaller capacity, resulting in higher hydrogen production costs. In both scenarios, the SOEC sector accounts for the second-highest proportion after nuclear power, indicating its substantial impact on hydrogen production costs. However, due to the nature of the process that converts electrical energy into hydrogen, electrolyzer systems are installed on a modular basis, regardless of reactor scale. Consequently, the cost difference between the two scenarios in the SOEC sector was less dramatic than in the nuclear sector. Meanwhile, the cost of the compression sector, which is required to pressurize the hydrogen to 70 bars, was found to account for only a very small proportion of the total LCOH.

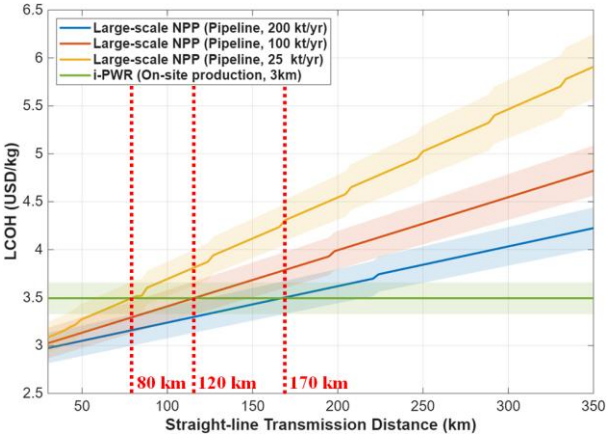

Figure 4. Break-even distance analysis of life-cycle LCOH between the large-scale NPP and i-PWR according to hydrogen demand scales.

Figure 4 compares LCOH for a large-scale NPP with a long-distance pipeline and a distributed production method with an i-PWR near the demand site (with a 3-km pipeline). These values were derived through Monte Carlo simulations for different demand scales (25, 100, and 200 kt/yr). The solid lines in the graph represent the average LCOH sampled 50,000 times. The surrounding translucent shaded areas indicate the 95% confidence interval, which reflects uncertainties in system capital costs and other variables.

The pipeline transmission scenarios for the large-scale NPP were subdivided according to annual hydrogen demand to quantitatively verify differences in transmission LCOH based on transport scale and economies of scale effects of pipeline infrastructure. The analysis results showed that, for a small-scale demand of 25 kt/yr (yellow solid line), the fixed cost of building the infrastructure significantly increases the LCOH per unit mass of hydrogen as the transmission distance increases, resulting in the steepest increase. Conversely, for a large-scale demand of 200 kt/yr (blue solid line), fixed infrastructure costs are distributed through mass transport via large-diameter pipes, resulting in a relatively moderate increase in LCOH. Additionally, the increases in steps observed in the pipeline transmission curves indicate cost increases caused by the installation of booster stations, which require additional compressors and intercoolers, to compensate for pressure drops due to pipe friction during long-distance transmission.

According to the break-even distance analysis, the i-PWR-based direct production method secures high price competitiveness compared to the large-scale NPP-based long-distance transmission method beyond a specific transmission distance. This method only performs short-distance pipeline transmission. Based on the average LCOH, the economic reversal occurs at approximately 80 km for a 25 kt demand, 120 km for a 100 kt demand, and 170 km for a 200 kt demand. Furthermore, the overlapping shaded regions of the 95% confidence intervals suggest statistical risk intervals in which the break-even distance could advance or delay depending on the variation of uncertain variables, such as initial investment costs.

The cost breakdown shows that large-scale NPPs have an initial production cost advantage of about 0.6 USD/kg-H_2. However, from a life-cycle LCOH perspective, this benefit is quickly offset by investments in pipeline infrastructure as transmission distance increases and demand decreases. Therefore, large-scale NPP deployment can be economically advantageous when utilizing large-diameter pipelines to maximize economies of scale. Conversely, for remote or small-to-medium-scale demand sites, where such extensive networks are impractical, an i-PWR-based distributed production system is a plausible alternative.

4. Conclusions & Future works

This study conducted a comprehensive life-cycle techno-economic assessment that compared hydrogen production systems integrating SOEC technology with either a centralized, large-scale NPP or a decentralized SMR (i-PWR). The thermodynamic analysis revealed that the large-scale NPP achieves a hydrogen production efficiency of about 34%, while the i-PWR achieves about 31%.

From an economic perspective, the cost breakdown revealed that large-scale NPPs have an initial production cost advantage of about 0.6 USD/kg-H_2 at the plant gate. This competitiveness is fundamentally driven by the strong economies of scale inherent in large nuclear facilities. However, life-cycle evaluation incorporating pipeline delivery revealed that this production advantage is quickly offset by the capital-intensive nature of long-distance transmission infrastructure. Break-even distance analysis demonstrated that the economic viability of each system is sensitive to transmission distance and target hydrogen demand. For a demand of 25 kt/yr, on-site i-PWR production is more economical than the large-scale NPP at a transmission distance of approximately 90 km. This break-even point extends to 130 km and 190 km for larger demands of 100 kt/yr and 200 kt/yr, respectively. Consequently, large-scale NPP deployment is primarily economically feasible when utilizing large-diameter pipelines that maximize economies of scale. In contrast, for remote or small-to-medium-scale demand centers, where extensive pipeline networks are impractical, deploying i-PWRs for decentralized hydrogen production is a highly competitive alternative because it eliminates long-distance transmission costs.

Despite providing quantitative insights, this study has several limitations that future research should address. First, the integrated thermodynamic modeling relies on steady-state assumptions and does not fully capture the transient, dynamic behavior of the actual coupled system. Additionally, the study did not explicitly model the performance degradation of the SOEC stacks over time,

which gradually reduces hydrogen production efficiency and necessitates varying thermal or electrical inputs. Future studies should incorporate dynamic simulation frameworks and empirical degradation rates to evaluate long-term operational stability.

Second, while Monte Carlo simulations were used to address uncertainties, baseline capital expenditures were primarily derived from literature values using a top-down approach. To improve the accuracy of the economic evaluation, subsequent research should conduct detailed, bottom-up cost estimations at the component level that reflect specific engineering designs and domestic market conditions.

Finally, the pipeline transmission model makes several assumptions. It simplifies fluid dynamics and uses a uniform factor to estimate the routing length. However, this approach neglects the significant impact of complex topographical variations, elevation changes, and transient flow phenomena on pressure drops and flow velocities within the pipe. To optimize actual routing and accurately quantify transmission requirements, future pipeline assessments should integrate geographic information system tools with advanced fluid dynamic simulations.

Acknowledgements

This work was supported by the Innovative Small Modular Reactor Development Agency grant funded by the Korea Government MOTIE (No. RS-2024-00400615)

Appendix

Appendix A. Hydrogen production cost

In the nuclear power generation cost model, total capital investment (TCI) was calculated by adding the overnight cost (OC) and interest during construction (IDC). O&M cost and fuel costs were estimated in proportion to annual electricity generation. In accordance with domestic nuclear regulatory standards, the model also incorporates decommissioning costs for nuclear facilities and management fees for low-, intermediate-, and high-level radioactive waste. Socio-political indirect costs, including subsidies for surrounding communities and taxes on local resources, were embedded in the estimation model as well.

Notably, this analysis clearly shows the differences in calculating social and post-operational costs based on reactor type. Calculations for large-scale nuclear power plants were performed using publicly available social cost data. Conversely, i-PWRs present a limitation due to the restricted availability of public information about their commercialization. To address this, the decommissioning and social costs of the i-PWR were estimated using a capacity-proportional scaling method based on the reference cost data of large-scale NPP. The specific economic parameters used in the model are detailed in Table 6–8.

Table 6. Economic parameters of the nuclear power plant

Parameter	Large-scale NPP (2020 USD) [13]	i-PWR 2022 USD [14]
Overnight Cost *	2157 USD/kWe	3500 USD/kWe
O&M Cost *	18.44 USD/MWh	28.96 USD/MWh
Construction Period	7 years	3 years
Interest Rate	5%	5%
Fuel Cost *	9.33 USD/MWh	10.3 USD/MWh
Capacity Factor	85%	

Table 7. Summary of decommissioning and radioactive waste management costs (2020 USD) [15]

Parameter		Large-scale NPP	i-PWR
Nuclear decommissioning cost (De) *		KRW 12,070 hundred million	KRW 3,406 hundred million
LILW	Unit cost	KRW 16,390,000 per drum	
	Annual generation	100 drums/year	12 drums/year
	Annual cost *	KRW 16.39 hundred million	KRW 1.97 hundred million
HLW	Unit cost	KRW 615,521,000 per fuel assembly	
	Total generation	4,175 fuel assemblies	507 fuel assemblies
	Annual cost *	KRW 428.3 hundred million	KRW 52.01 hundred million

Table 8. Parameters for policy-based indirect costs and regional subsidies (2020 USD) [16]

Parameter	Large-scale NPP	i-PWR
Neighboring-area Assistance Subsidy	0.25 KRW/KWh	
Local Resource and Facility Tax	1 KRW/KWh	
Host-area Support for a Radioactive Waste Disposal Facility	KRW 248.6 billion	KRW 70.16 billion

Transmission Connection Charge	1.02 KRW/KWh	X

Parameters marked with an asterisk (*) were assumed to follow a triangular distribution with a ±20% uncertainty margin for the Monte Carlo simulation. The CAPEX for the SOEC system was determined using the required system capacity, which was derived in Section 2.1. Rather than relying on simple linear scaling, the TCI was evaluated using a cost correlation method developed by the Idaho National Laboratory. This analytical model calculates the specific capital cost as a function of plant capacity (P_{EL}), distinguishing the economic contributions of scalable and modular equipment components.

$$TCI_{SOEC} = m(a_{scalable}P^{n_{scalable}} + a_{modular}P^{n_{modular}}) \quad (10)$$

To reflect the initial phase of commercial deployment, the correlation parameters corresponding to the first-of-a-kind (FOAK) plant type were applied. The specific TCI parameters, as well as the base stack cost and operation and maintenance expenditures calibrated to South Korean labor standards, are compiled in Table 9 and 10.

Table 9. SOEC TCI correlation parameters * (FOAK, 2020 USD) [10]

Parameter	Value
SOEC stack cost	$155 / kW-dc
m	1.2383
$a_{scalable}$	799.1
$n_{scalable}$	-0.505
$a_{modular}$	596.4
$n_{modular}$	-0.043

Table 10. O&M assumptions for hydrogen production plant

Parameter	Value
Total Plant Staff [17]	16 (corresponds to 800 tonne/day design hydrogen production capacity)
Burdened labor cost	$16.87/hr
G&A rate/costs [18]	20% of labor
Property tax and insurance [18]	2% of TCI_{EL} per year
Production maintenance and repair [18]	3% of DCC_{EL} per year

Appendix B. Hydrogen compression cost

$$CAPEX_{compressor}[2013\$] = 1.3 \times 40528 \times (n_{working} + n_{backup}) \times MR^{0.4603} \quad (11)$$

Intercooler CAPEX was evaluated using the shell-and-tube heat exchanger economic methodology proposed by Turton et al. [19]. The foundational purchase cost (C_B^0) is derived from the heat transfer area (A_{HX}), according to Eq. (12). This base value is then adjusted using material (F_M) and pressure (F_P) correction factors to yield the final installed cost ($CAPEX_{intercooler}$) as detailed in Eq. (13,14). A comprehensive summary of these critical design variables is provided in Table 11.

$$\log_{10} C_B^0 = K_1 + K_2 \cdot \log_{10} A_{HX} + K_3 \cdot (\log_{10} A_{HX})^2 \quad (12)$$

$$\log_{10} F_P = C_1 + C_2 \cdot \log_{10} P + C_3 \cdot (\log_{10} P)^2 \quad (13)$$

$$CAPEX_{intercooler} = C_B^0(B_1 + B_2 F_M F_P) \quad (14)$$

Table 11. Input parameters for the compression system model [12]

Parameter	Value
Safety / service factor (SF)	1.1
Working compressors	2 units
Backup compressors	1 unit
Design lifetime (N)	15 years
O&M cost (O&M)	4% of CAPEX per year
HX type	STHE

Appendix C. Hydrogen transmission cost

The economic assessment of pipeline delivery includes the CAPEX for pipeline installation, determined by a diameter-specific unit cost. It also includes the cost of procuring booster compressors, if necessary, to overcome pressure drops. Regarding hydrogen loss during delivery, permeation through the pipeline wall is considered negligible and thus ignored. However, a mass loss of 0.5% is assumed for each booster compressor stage due to dynamic seal leakage and venting [20]. The estimated actual routing length of the pipeline was calculated by multiplying the straight-line distance between the production and demand nodes by a tortuosity factor of 1.4. The electricity required to operate the compressors is assumed to be drawn from the electricity grid, and the associated costs were calculated using the average SMP in 2024.

The economic parameters that govern the pipeline transmission strategy are presented in Table 12.

Consistent with the cost evaluation of the previous components, the PV of all periodic replacement and operational expenses for the transmission equipment over the nuclear power plant's operational lifetime were calculated and included in the final life-cycle LCOH.

Table 12. Pipeline unit capital costs [21]

Diameter (inch)	Unit CAPEX (million USD/mile) (2024 USD)*	Unit CAPEX (million USD/mile) (ref, 2008 USD)
4	1.18	0.58
6	2.44	1.2
8	4.06	2
12	6.9	3.4
16	9.54	4.7
20	12.0	5.9

Table 13. Economic parameters used for transmission cost model [12, 22]

Parameter	Value
Pipeline lifetime	60 years
$O\&M_{\text{pipe}}$	$2.5\% \times CAPEX_{\text{pipe}}$
SMP (2024, Korea)	128.39 won/kWh

REFERENCES

[1] International Energy Agency (IEA), "Global Hydrogen Review 2023," IEA, Paris, France, 2023. [Online]. Available: https://www.iea.org/reports/global-hydrogen-review-2023
[2] Ministry of Trade, Industry and Energy (MOTIE), "Hydrogen Economy Roadmap of Korea," Gov. of the Republic of Korea, Seoul, South Korea, Jan. 2019.
[3] "Hydrogen Economy Promotion and Hydrogen Safety Management Act," Act No. 16942, Republic of Korea, Feb. 2020.
[4] International Atomic Energy Agency (IAEA), "Examining the Technoeconomics of Nuclear Hydrogen Production and Benchmark Analysis of the IAEA HEEP Software," IAEA, Vienna, Austria, IAEA-TECDOC-1859, 2018.
[5] M. A. Pearsall et al., "Water Electrolysis Technologies and Their Modeling Approaches: A Comprehensive Review," Clean Technol., vol. 6, no. 4, p. 81, 2024
[6] Clean Air Task Force (CATF), "Solid Oxide Electrolysis: A Technology Status Assessment," CATF, Nov. 2023. [Online]. Available: https://www.catf.us/resource/solid-oxide-electrolysis-technology-status-assessment/
[7] International Energy Agency (IEA), "The Future of Hydrogen: Seizing today's opportunities," IEA, Paris, France, 2019.
[8] "APR1400 DESIGN CONTROL DOCUMENT TIER 2 CHAPTER 10 STEAM AND POWER CONVERSION SYSTEM," 2018.
[9] L. NuScale Power, "Part 02 - Final Safety Analysis Report (Rev. 5) - Part 02 - Tier 02 - Chapter 10 - Steam and Power Conversion System - Sections 10.01 - 10.04."
[10] L. T. Knighton *et al.*, "Techno-economic analysis of product diversification options for sustainability of the Monticello and Prairie Island nuclear power plants," Idaho National Lab. (INL), Idaho Falls, ID, USA, Rep. INL/EXT-21-62563-Rev001, 2021.
[11] K. Petak, H. Vidas, J. Manik, S. Palagummi, A. Ciatto, and A. Griffith, "INFRASTRUCTURE INVESTMENT AN ENGINE FOR ECONOMIC GROWTH STUDY PREPARED FOR AMERICAN PETROLEUM INSTITUTE ICF Authors," 2017.
[12] "HYDROGEN DELIVERY SCENARIO ANALYSIS MODEL (HDSAM)," *UChicago Argonne*. Accessed: Jan. 05, 2026. [Online]. Available: https://hdsam.es.anl.gov/
[13] "Projected Costs of Generating Electricity," 2020.
[14] 신재정, 김창훈, "소형모듈형원전 기술과 산업 경쟁력 강화 방안 연구(2/3)," 2024.
[15] *Guideline on the Calculation of Electric Power Generation Costs, etc.*, Ministry of Trade, Industry and Energy Notification No. 2024-94, Sejong, South Korea, May 31, 2024.
[16] Korea Power Exchange (KPX) and Korea Energy Economics Institute (KEEI), "Levelized cost of electricity by power source," Naju, South Korea, Tech. Rep., Dec. 2018.
[17] K. Randolph, N. Stetson, S. Satyapal, and L. Value, "DOE Hydrogen and Fuel Cells Program Record 20006: Hydrogen Production Cost from High Temperature Electrolysis," 2020.
[18] D. S. Wendt, L. T. Knighton, and R. D. Boardman, "High-Temperature Steam Electrolysis Process Performance and Cost Estimates," 2022.
[19] R. Turton, R. C. Bailie, W. B. Whiting, J. A. Shaeiwitz, and D. Bhattacharyya, *Analysis, Synthesis, and Design of Chemical Processes*, 5th ed. Upper Saddle River, NJ, USA: Pearson, 2018.
[20] U.S. Department of Energy (DOE), "Multi-Year Research, Development, and Demonstration Plan: Section 3.2 Hydrogen Delivery," Fuel Cell Technologies Office, Washington, D.C., USA, 2015.
[21] Nexant, "H2A Hydrogen Delivery Infrastructure Analysis Models and Conventional Pathway Options Analysis Results," 2008.
[22] Korea Power Exchange (KPX), "Settlement Unit Price by Energy Source," *Electric Power Statistics Information System (EPSIS)*, Naju, South Korea, 2025.